

## Investigation of E1(LO) phonon-plasmon coupled modes and critical points in In<sub>1-x</sub>Ga<sub>x</sub>N thin films by optical reflectance measurements

J. S. Thakur, A. Dixit, Y. V. Danylyuk, C. Sudakar, V. M. Naik et al.

Citation: *Appl. Phys. Lett.* **96**, 181904 (2010); doi: 10.1063/1.3428368

View online: <http://dx.doi.org/10.1063/1.3428368>

View Table of Contents: <http://apl.aip.org/resource/1/APPLAB/v96/i18>

Published by the [American Institute of Physics](http://www.aip.org).

---

### Additional information on *Appl. Phys. Lett.*

Journal Homepage: <http://apl.aip.org/>

Journal Information: [http://apl.aip.org/about/about\\_the\\_journal](http://apl.aip.org/about/about_the_journal)

Top downloads: [http://apl.aip.org/features/most\\_downloaded](http://apl.aip.org/features/most_downloaded)

Information for Authors: <http://apl.aip.org/authors>

## ADVERTISEMENT

**AIP** | Applied Physics  
Letters

**EXPLORE WHAT'S NEW IN APL**

**SUBMIT YOUR PAPER NOW!**

**SURFACES AND INTERFACES**  
Focusing on physical, chemical, biological, structural, optical, magnetic and electrical properties of surfaces and interfaces, and more...

**ENERGY CONVERSION AND STORAGE**  
Focusing on all aspects of static and dynamic energy conversion, energy storage, photovoltaics, solar fuels, batteries, capacitors, thermoelectrics, and more...

Labels in diagram: 1µm-thick LPCVD Silicon Dioxide, Source, Drain, Metal Vias, Ground Ring.

# Investigation of $E_1(\text{LO})$ phonon-plasmon coupled modes and critical points in $\text{In}_{1-x}\text{Ga}_x\text{N}$ thin films by optical reflectance measurements

J. S. Thakur,<sup>1,a)</sup> A. Dixit,<sup>1</sup> Y. V. Danylyuk,<sup>2</sup> C. Sudakar,<sup>1</sup> V. M. Naik,<sup>3</sup> W. J. Schaff,<sup>4</sup> and R. Naik<sup>1</sup>

<sup>1</sup>Department of Physics and Astronomy, Wayne State University, Detroit, Michigan 48202, USA

<sup>2</sup>Department of Electrical and Computer Engineering, Wayne State University, Detroit, Michigan 48202, USA

<sup>3</sup>Department of Natural Sciences, University of Michigan–Dearborn, Dearborn, Michigan 48128, USA

<sup>4</sup>Department of Electrical and Computer Engineering, Cornell University, Ithaca, New York 14853, USA

(Received 8 February 2010; accepted 15 April 2010; published online 6 May 2010)

Low energy optical modes of molecular beam epitaxy-grown  $\text{In}_{1-x}\text{Ga}_x\text{N}$  thin films with  $0 \leq x \leq 0.6$  are investigated using infrared reflectance measurements. We found that the reflectance of the films for wave vectors in the range from 600 to 800  $\text{cm}^{-1}$  is determined by the high energy  $E_1(\text{LO})$ -plasmon coupled modes. In the higher energy regime of the UV-visible reflectance spectrum of InN, critical points with energies 4.75, 5.36, and 6.12 eV belonging to A and B structures are observed. The energies of these critical points increase with increasing values of  $x$ , similar to the band gap energy of these films. © 2010 American Institute of Physics. [doi:10.1063/1.3428368]

Indium nitride (InN) and gallium nitride (GaN) are important electronic materials among various III-nitride semiconductors with numerous applications in the areas of lasers, photovoltaic devices, infrared (IR), visible, and ultraviolet (UV) detectors, etc.<sup>1</sup> However, the band gap energy of InN thin film materials<sup>2–6</sup> is still controversial.  $\text{In}_{1-x}\text{Ga}_x\text{N}$  materials offer a possibility of tuning band gap from near-IR (NIR) to UV regimes. Given the numerous applications of  $\text{In}_{1-x}\text{Ga}_x\text{N}$  semiconductors in optical devices, it is important to investigate the phonon spectra of these materials in the IR region. In particular, the longitudinal optical (LO) components of  $E_1$  and  $A_1$  phonons play a dominant role in the electron scattering processes and can also couple with the plasmon oscillations creating plasmon-phonon coupled modes.<sup>7,8</sup> Coupling of  $A_1(\text{LO})$  phonon with plasmon has been extensively studied for InN films using Raman spectroscopy.<sup>7,9</sup>

$\text{In}_{1-x}\text{Ga}_x\text{N}$  thin films were prepared by molecular beam epitaxy technique at Cornell University.<sup>4,5</sup> Thin buffer layers of AlN and GaN with thickness  $\sim 10$  and 220 nm were grown to reduce the lattice mismatch between  $\text{In}_{1-x}\text{Ga}_x\text{N}$  thin films and c-sapphire substrate. The interference fringe width from UV-vis-NIR reflection spectrum was used to estimate the thickness of these thin films which varied from 0.4 to 0.6  $\mu\text{m}$ . The room temperature carrier concentration,  $N_e$ ,

Hall mobility, and band gap energy (determined from optical transmittance and reflectance spectra) are listed in Table I.

Figure 1 shows the IR reflectance spectra of  $\text{In}_{1-x}\text{Ga}_x\text{N}$  thin films and sapphire substrate measured using normal incidence configuration. Due to small thickness of the  $\text{In}_{1-x}\text{Ga}_x\text{N}$  layer in the films, a significant fraction of the light reaches the sapphire surface and reflects back. The overall profile of the reflectance spectra for wave vectors less than 600  $\text{cm}^{-1}$  and dips at 390 and 630  $\text{cm}^{-1}$  can be easily associated with the reflectance from sapphire IR-phonons. The bottom panel in Fig. 1 shows the IR reflectance for InN film. Most of the spectral features observed in the  $\text{In}_{0.85}\text{Ga}_{0.15}\text{N}$  film are the same as that of the InN film. However, for larger  $x$  some noticeable changes occur in the spectra (see  $\text{In}_{0.70}\text{Ga}_{0.30}\text{N}$  and  $\text{In}_{0.46}\text{Ga}_{0.54}\text{N}$ ). For example, the position of the dip observed in InN film at 445  $\text{cm}^{-1}$  associated with  $E_1(\text{TO})$  mode increases with increasing  $x$  and so is its broadening indicating an increase in the disorder of the  $\text{In}_{1-x}\text{Ga}_x\text{N}$  films. The calculated values of plasmon frequency,  $\omega_p = \sqrt{4\pi N_e e^2 / (\epsilon_\infty m_e^*)}$ , ( $m_e^*$  is electron's effective mass and  $\epsilon_\infty$  is dielectric constant) are very close to the  $E_1(\text{LO})$ -phonon frequency,  $\omega_{\text{LO}}$ , (see Table I), and hence one expects a strong influence of the plasmon-phonon coupling. We have calculated the reflectance of the  $\text{In}_{1-x}\text{Ga}_x\text{N}$  layer using a dielectric function,<sup>9</sup>

TABLE I. Electronic and optical properties of  $\text{In}_{1-x}\text{Ga}_x\text{N}$  thin films for different values of  $x$ .

Sample	$N_e$ ( $\text{cm}^{-3}$ )	$\mu$ ( $\text{cm}^2/\text{V s}$ )	$E_g$ (eV)	$\omega_{\text{LO}}$ ( $\text{cm}^{-1}$ )	$\omega_p$ ( $\text{cm}^{-1}$ )	$\omega_+$ ( $\text{cm}^{-1}$ )	$\omega_-$ ( $\text{cm}^{-1}$ )
InN	$1.3 \times 10^{18}$	900	0.77	600	562	737	366
$\text{In}_{0.85}\text{Ga}_{0.15}\text{N}$	$1.4 \times 10^{18}$	700	0.96	621	586	767	374
$\text{In}_{0.70}\text{Ga}_{0.30}\text{N}$	$2.3 \times 10^{18}$	140	1.27	642	716	869	412
$\text{In}_{0.46}\text{Ga}_{0.54}\text{N}$	$1.1 \times 10^{18}$	20	1.85	654	522	781	344

<sup>a)</sup>Author to whom correspondence should be addressed. Electronic mail: jagdish@wayne.edu.

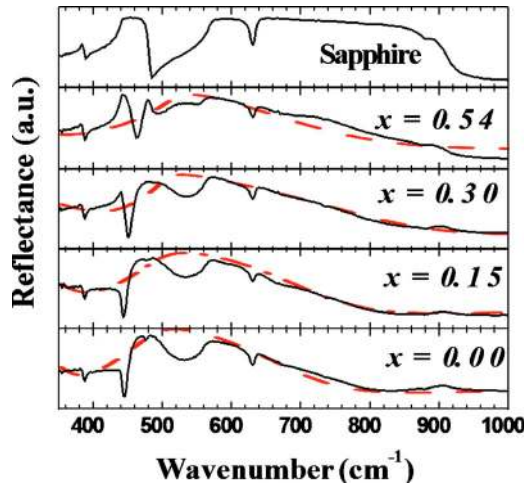


FIG. 1. (Color online) IR reflectance spectra of  $\text{In}_{1-x}\text{Ga}_x\text{N}$  ( $x=0, 0.15, 0.30$ , and  $0.54$ ) thin films under normal incidence. The dashed curves show the theoretical reflectance.

$$\varepsilon(\omega) = \varepsilon_\infty \frac{(\omega^2 - \omega_+^2 + i\gamma_+\omega)(\omega^2 - \omega_-^2 + i\gamma_-\omega)}{(\omega^2 + i\gamma_P\omega)(\omega^2 - \omega_{\text{TO}}^2 + i\gamma_{\text{TO}}\omega)}. \quad (1)$$

Here,  $\omega_i/\gamma_i$  ( $i=+, -, \text{TO}$ , and  $P$ ) represents energy/broadening constant for the coupled modes,  $E_1(\text{TO})$  phonon, and plasmon, respectively. The energies of the lower ( $\omega_-$ ) and higher ( $\omega_+$ ) coupled modes can be calculated from  $\omega_\pm = \sqrt{0.5[\omega_P^2 + \omega_{\text{LO}}^2 \pm \sqrt{(\omega_P^2 + \omega_{\text{LO}}^2)^2 - 4\omega_P^2\omega_{\text{TO}}^2}]^{1/2}}$ . The energies of these coupled modes (Table I) are affected by plasmon energy and also by the energies of  $\omega_{\text{LO}}$  and  $\omega_{\text{TO}}$  modes which change with  $x$ .

Figure 2 shows the variations in the energies of  $\omega_+$ ,  $\omega_-$ , and  $\omega_P$  as a function of  $N_e$  and also the values of these modes (solid circles) for two different values of  $x$ . The values of  $\omega_{\text{LO}}$  are steadily increasing with  $x$  in  $\text{In}_{1-x}\text{Ga}_x\text{N}$  films and so are the values of  $\omega_{\text{TO}} = \omega_{\text{LO}}\sqrt{\varepsilon_\infty(x)/\varepsilon_0}$  estimated from Lyddane–Sachs–Teller relation. Here  $\varepsilon_\infty(x)$  is calculated using  $\varepsilon_\infty(x) = \varepsilon_\infty^{\text{InN}}(1-x) + \varepsilon_\infty^{\text{GaN}}x$  with dielectric constants of InN,  $\varepsilon_\infty^{\text{InN}}=6.7$ , and GaN,  $\varepsilon_\infty^{\text{GaN}}=5.6$ . Increasing  $\omega_{\text{LO}}$  influences the high energy coupled mode more strongly than the lower energy coupled mode. When Ga concentration is uniformly increased in these films, we observe only small changes in the carrier density (Table I) which does not seem to be related to the variation in the values of  $x$ . However, the observed changes in the calculated values of  $\omega_P$  is due to small variations in the values  $N_e$ ,  $m_e^*$ , and  $\varepsilon_\infty$  with  $x$ . Furthermore, the interaction between  $\omega_P$  and  $E_1(\text{LO})$  does not change much with  $x$  due to small variation in the values of  $\varepsilon_\infty(x)$ .

One expects reflectance edges in the reflectance spectra at  $\omega_-$  and  $\omega_+$ , if the defect concentration is small. In our films, due to the presence of donor type of charged defects,<sup>6</sup> as reflected through the observed high  $N_e$  values, the plasmon mode is relatively heavily damped than the phonon mode. The spectral features of the reflectance spectra near the lower energy coupled mode region are dominated by the sapphire. However, for wave vectors ranging from 600 to 800  $\text{cm}^{-1}$ , the overall observed features of the reflectance spectra can be understood in terms of reflectance by the higher energy coupled mode as shown by the calculated plasmon- $E_1(\text{LO})$  phonon reflectance in the Fig. 1. Using

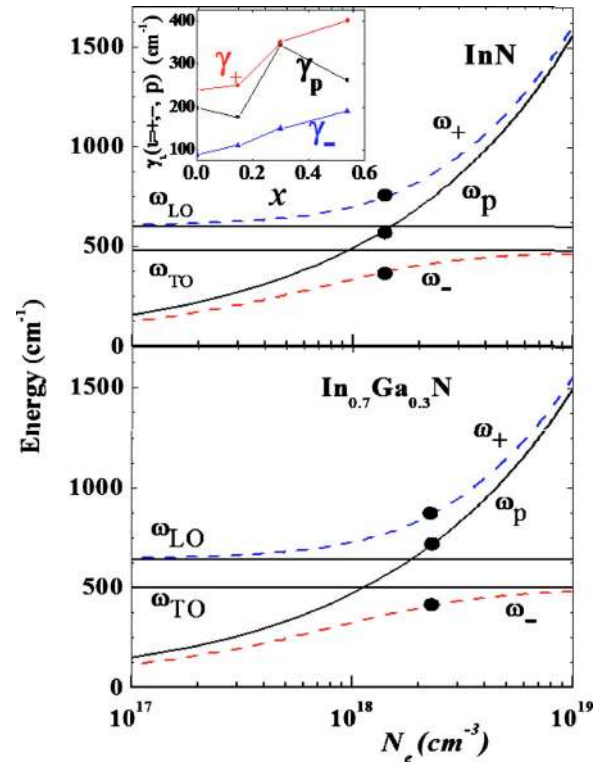


FIG. 2. (Color online) Variation in the energy of coupled modes and  $\omega_P$  with  $N_e$ . The energies of the coupled modes and plasmon for InN film and  $\text{In}_{0.7}\text{Ga}_{0.3}\text{N}$  are shown by the filled circles. Two straight lines in each panel represent the energies of  $\omega_{\text{LO}}$  and  $\omega_{\text{TO}}$  for the corresponding film. Inset shows variation in the broadening parameters,  $\gamma_+$ ,  $\gamma_-$ , and  $\gamma_P$ , with  $x$ .

Eq. (1), the calculated reflectance for each sample is shown by the dotted line. The spectral features of the reflectance are determined by the energies and their damping parameters of the modes. For the calculation of  $\omega_P$ , since the values of  $m_e^*$  for InGaN alloys are not very well known, we have used  $m_e^*$  ( $N_e$  dependent) of InN films.<sup>4</sup> However, larger  $m_e^*$  values (expected for InGaN alloys) slightly decrease the reflectance values, e.g., the calculated reflectance at the higher energy coupled mode's energy decreases by less than 5.0% when  $m_e^*$  is increased by 50%. As the value of  $x$  increases, the overall features of the reflectance remain roughly the same. Increasing values of  $x$  from 0.15 to 0.30 also increase disorder in the films as seen through the broadening of the spectral features in the reflectance spectra. The inset of Fig. 2 shows variations in  $\gamma_+$ ,  $\gamma_-$ , and  $\gamma_P$  as a function of  $x$ . Although the lower energy coupled mode is not very well seen in the reflectance spectra due to the dominance of the sapphire, the broadening parameter  $\gamma_-$  used in the fitting of the data is found to increase with  $x$ . For films with  $x=0.0, 0.15$ , and  $0.54$ , the values of  $\gamma_P$  do not change much because the carrier density is roughly the same. At  $x=0.30$ , carrier density is the highest and so is the plasmon scattering rate. The broadening factor  $\gamma_+$  shows a jump when  $x$  is increased from 0.15 to 0.30 which is consistent with the broadening observed in the measured reflectance in the 600 to 800  $\text{cm}^{-1}$  region. Its value further increases as  $x$  increases to 0.54 due to increase in lattice disorder caused by Ga.

High energy reflectance in the UV-visible region can also be used to investigate band structure properties of a material. In fact the characteristic structures, like the peaks and shoulders in a reflectance spectrum, are related to the

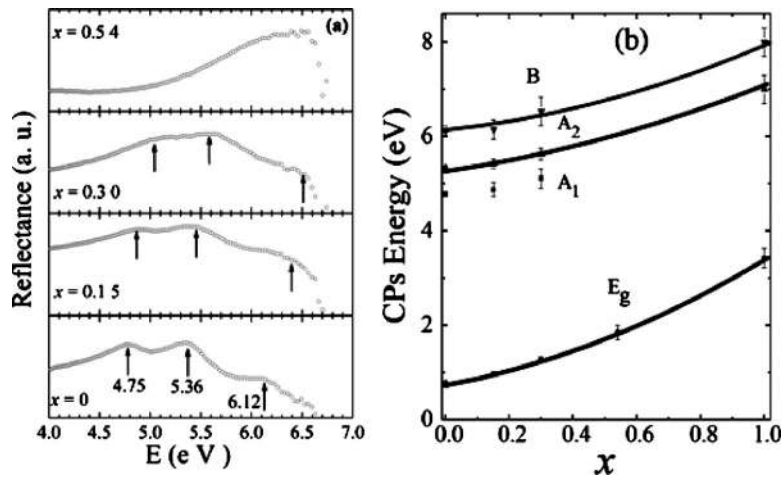


FIG. 3. (a) UV reflectance from  $\text{In}_{1-x}\text{Ga}_x\text{N}$  films showing the critical point transitions (shown by arrows) and (b) variation in critical point energies of  $\text{In}_{1-x}\text{Ga}_x\text{N}$  alloy as a function of  $x$ . The solid lines show the fitted data.

optical transitions at the critical points (CPs) of the energy difference between the initial and final energy bands involved in the excitation process. In order to investigate the CPs in our  $\text{In}_{1-x}\text{Ga}_x\text{N}$  films, we have measured reflectance over a very wide energy range for each film. These transitions are normally studied using synchrotron radiation.<sup>10</sup> In our reflectance spectra [Fig. 3(a)], we have observed two main transition structures known as A and B for wurtzite nitrides. For the structure A, two very well defined peaks with energies 4.75 and 5.36 eV are observed. While in the structure B, at least one critical point at 6.12 eV can be easily resolved. The energies of these critical points agree very well with the empirical pseudopotential method calculations<sup>11</sup> and ellipsometric measurements<sup>12</sup> on InN films. As the Ga content increases in  $\text{In}_{1-x}\text{Ga}_x\text{N}$  films, the energies of these critical points increase as shown in Fig. 3(b). These points can be fitted with an equation  $E_i(x) = E_i(\text{GaN})x + E_i(\text{InN})(1-x) - b_i x(1-x)$ , where the subscript  $i$  represents a CP transition and  $b_i$  the corresponding bowing parameter.  $E_i(\text{GaN})$  and  $E_i(\text{InN})$  are the transition energies for the  $i$ th type of transition of GaN and InN films, respectively. From the energies of A (7.0 eV) and B (8.0 eV) transition structures<sup>13</sup> for GaN, we estimated the corresponding  $b_i$  parameters for the  $\text{In}_{1-x}\text{Ga}_x\text{N}$  films and found their values  $b_{A2} = 1.11 \pm 0.21$  eV and  $b_B = 1.26 \pm 0.70$  eV. The energies of the critical points vary monotonically with increasing values of  $x$ , similar to the band gap energy of these films. The curve at the bottom represents the variation in the energy of the direct band gap generated using  $E_g(\text{GaN}) = 3.42$  eV,  $E_g(\text{InN}) = 0.77$  eV, and  $b_{Eg} = 1.44 \pm 0.12$  eV for the  $\text{In}_{1-x}\text{Ga}_x\text{N}$  films.<sup>5</sup>

In summary, we investigated the low energy optical phonons of  $\text{In}_{1-x}\text{Ga}_x\text{N}$  thin films using IR reflectance measurements. We found that the higher energy plasmon- $E_1(\text{LO})$

phonon coupled mode strongly influences the reflectance spectra of the films. Using reflectance spectroscopy in the energy range from 4.0 to 7.0 eV we have also investigated the critical points of  $\text{In}_{1-x}\text{Ga}_x\text{N}$  band structure. We observe three critical points in this energy range and they are in agreement with the theoretically predicted values.

The authors would like to acknowledge the Richard Barber Funds for interdisciplinary Research and thank Dr. Gavin Lawes for useful discussions.

- <sup>1</sup>S. C. Jain, M. Willander, J. Narayan, and R. V. Overstraeten, *J. Appl. Phys.* **87**, 965 (2000).
- <sup>2</sup>J. Wu and W. Walukiewicz, *Superlattices Microstruct.* **34**, 63 (2003).
- <sup>3</sup>A. Dixit, C. Sudakar, R. Naik, G. Lawes, J. S. Thakur, E. F. McCullen, G. W. Auner, and V. M. Naik, *Appl. Phys. Lett.* **93**, 142103 (2008).
- <sup>4</sup>J. Wu, W. Walukiewicz, W. Shan, K. M. Yu, J. W. Ager III, E. E. Haller, H. Lu, and W. J. Schaff, *Phys. Rev. B* **66**, 201403(R) (2002).
- <sup>5</sup>J. Wu, W. Walukiewicz, K. M. Yu, J. W. Ager III, E. E. Haller, H. Lu, and W. J. Schaff, *Appl. Phys. Lett.* **80**, 4741 (2002).
- <sup>6</sup>J. S. Thakur, Y. V. Danylyuk, D. Haddad, V. M. Naik, R. Naik, and G. W. Auner, *Phys. Rev. B* **76**, 035309 (2007).
- <sup>7</sup>J. S. Thakur, D. Haddad, V. M. Naik, R. Naik, G. W. Auner, H. Lu, and W. J. Schaff, *Phys. Rev. B* **71**, 115203 (2005).
- <sup>8</sup>J. S. Thakur, G. W. Auner, D. B. Haddad, R. Naik, and V. M. Naik, *J. Appl. Phys.* **95**, 4795 (2004).
- <sup>9</sup>A. Kasic, M. Schubert, Y. Saito, Y. Nanishi, and G. Wagner, *Phys. Rev. B* **65**, 115206 (2002).
- <sup>10</sup>R. Goldhahn, P. Schley, A. T. Winzer, M. RakeI, C. Cobet, N. Esser, H. Lu, and W. J. Schaff, *J. Cryst. Growth* **288**, 273 (2006).
- <sup>11</sup>D. Fritsch, H. Schmidt, and M. Grundmann, *Phys. Rev. B* **69**, 165204 (2004).
- <sup>12</sup>A. Kasic, E. Valcheva, B. Monemar, H. Lu, and W. J. Schaff, *Phys. Rev. B* **70**, 115217 (2004).
- <sup>13</sup>T. Kawashima, H. Yoshikawa, S. Adachi, S. Fuke, and K. Ohtsuka, *J. Appl. Phys.* **82**, 3528 (1997).